IGF-1 degradation by mouse mast cell protease 4 promotes cell death and adverse cardiac remodeling days after a myocardial infarction

Thor Tejada[a,1], Lin Tan[a,1], Rebecca A. Torres[a], John W. Calvert[b], Jonathan P. Lambert[b], Madiha Zaidi[a], Murtaza Husain[a], Maria D. Berce[a], Hussain Naib[a], Gunnar Pejler[c,d], Magnus Abrink[e], Robert M. Graham[f], David J. Lefer[b], Nawazish Naqvi[a,2], and Ahsan Husain[a,2]

[a]Department of Medicine (Cardiology), Emory University School of Medicine, Atlanta, GA 30322; [b]Department of Surgery (Carlyle Fraser Heart Center), Emory University School of Medicine, Atlanta, GA 30322; [c]Department of Medical Biochemistry and Microbiology, Uppsala University, Uppsala, Sweden; [d]Department of Anatomy, Physiology and Biochemistry, Swedish University of Agricultural Sciences, Uppsala, Sweden; [e]Department of Biomedical Sciences and Veterinary Public Health, Swedish University of Agricultural Sciences, Uppsala, Sweden; and [f]Victor Chang Cardiac Research Institute, Sydney, NSW 2010, Australia

Edited by Christine E. Seidman, Howard Hughes Medical Institute, Harvard Medical School, Boston, MA, and approved May 2, 2016 (received for review February 24, 2016)

Heart disease is a leading cause of death in adults. Here, we show that a few days after coronary artery ligation and reperfusion, the ischemia-injured heart elaborates the cardioprotective polypeptide, insulin-like growth factor-1 (IGF-1), which activates IGF-1 receptor prosurvival signaling and improves cardiac left ventricular systolic function. However, this signaling is antagonized by the chymase, mouse mast cell protease 4 (MMCP-4), which degrades IGF-1. We found that deletion of the gene encoding MMCP-4 (*Mcpt4*), markedly reduced late, but not early, infarct size by suppressing IGF-1 degradation and, consequently, diminished cardiac dysfunction and adverse structural remodeling. Our findings represent the first demonstration to our knowledge of tissue IGF-1 regulation through proteolytic degradation and suggest that chymase inhibition may be a viable therapeutic approach to enhance late cardioprotection in post-ischemic heart disease.

insulin-like growth factor-1 | chymase | mouse mast cell protease 4 | ischemia-reperfusion injury | cardioprotection

Drugs that inhibit angiotensin II (Ang II) action or formation reduce mortality and cardiovascular morbidity in patients with myocardial infarction (MI) complicated by left ventricle (LV) systolic dysfunction, heart failure, or both (1, 2). Because human chymase, a mast cell protease (3), is an Ang II-forming enzyme (4) it is thought that, like angiotensin I-converting enzyme (ACE), chymase might be a useful drug target in the therapy of post-MI patients. However, the Valsartan in Acute Myocardial Infarction (VALIANT) trial, comparing inhibition of ACE with angiotensin receptor subtype-1 blockade (ARB), did not support a role for alternate Ang II-generating pathway(s) in post-MI heart failure (2).

In rodents, chymase inhibitor monotherapy improved survival and reduced post-MI cardiac hypertrophy and dysfunction (5, 6). Although these studies, and clinical trials, together suggest an Ang II-independent mechanism of action of chymase inhibitors, other studies with chymase inhibitor monotherapy were negative (7, 8). Variations in the specificities of chymase inhibitors—that were designed to inhibit human chymase—could be a source of differences in outcomes when used in nonprimates. This uncertainty led us to reassess whether chymase is an important therapeutic target for improving structure and function in ischemia-injured hearts by using a genetic model that obviates the issue of inhibitor specificity.

Mouse mast cell protease 4 (MMCP-4) is the functional homolog of human chymase (8). To address its role in post-MI hearts, we used mice lacking *Mcpt4*, the gene encoding MMCP-4. We show that 2 wk after cardiac ischemia and then reperfusion (I/R), beneficial effects of *Mcpt4* deletion occur even after renin–angiotensin system (RAS) blockade. Thus, MMCP-4 inhibition may have therapeutic effects beyond those of mere RAS blockade. Specifically, we discovered that MMCP-4 is an insulin-like growth factor-1 (IGF-1)–degrading enzyme and that beneficial effects of *Mcpt4* deletion involve sustained IGF-1 levels and IGF-1 receptor (IGF-1R) prosurvival signaling after I/R.

IGF-1 is highly cardioprotective in the setting of permanent coronary artery occlusion or I/R (9). A single intracoronary artery dose of IGF-1 in dogs after I/R reduces cardiomyocyte apoptosis within the ischemic border zone (10), and intramyocardial IGF-1 administration reduces post-MI infarct size and LV dysfunction in rats (11). However, dose-dependent side effects of acute or chronic IGF-1 therapy, which include potentially maladaptive promotion of cardiomyocyte hypertrophy (12), have hampered its clinical usefulness as a therapy. Hence, our findings open a previously unidentified avenue for locally increasing the cardioprotective effects of IGF-1 signaling by inhibiting a protease that regulates its degradation without impacting circulating IGF-1 levels.

Significance

Coronary heart disease is a leading cause of death worldwide. After acute myocardial infarction, early reperfusion limits infarct progression and improves clinical outcomes. However, despite reperfusion, the incidence of heart failure and cardiovascular deaths remains unacceptably high. Here, we report that a few days after ischemia, the reperfused heart transiently elaborates the cardioprotective polypeptide, insulin-like growth factor-1 (IGF-1). However, tissue IGF-1 levels increase only transiently because it is rapidly degraded by the chymase, mouse mast cell protease 4. Mouse mast cell protease 4 deletion promotes cardiac cell survival by reducing IGF-1 degradation, which ameliorates cardiac dysfunction caused by ischemic injury. Our findings suggest that chymase inhibition may be a viable therapeutic approach to enhance late cardioprotection in post-ischemic heart disease.

Author contributions: T.T., D.J.L., N.N., and A.H. designed research; T.T., L.T., R.A.T., J.W.C., J.P.L., M.Z., M.H., M.D.B., H.N., and N.N. performed research; G.P. and M.A. contributed new reagents/analytic tools; A.H. analyzed data; and R.M.G., D.J.L., N.N., and A.H. wrote the paper.

The authors declare no conflict of interest.

This article is a PNAS Direct Submission.

Freely available online through the PNAS open access option.

[1]T.T. and L.T. contributed equally to this work.

[2]To whom correspondence may be addressed. Email: ahusai2@emory.edu or nnaqvi@emory.edu.

This article contains supporting information online at www.pnas.org/lookup/suppl/doi:10.1073/pnas.1603127113/-/DCSupplemental.

Results

MMCP-4 Promotes Post-I/R Cardiac Dysfunction and Remodeling. MMCP-4 protein and mRNA were low in uninjured hearts (Fig. 1 *A*–*C*). Thereafter, MMCP-4 protein and mRNA levels increased, with the highest levels observed at 72 h of reperfusion (Fig. 1 *A* and *B*). Mast cells contain a number of preformed chemical mediators such as histamine, chymase, carboxypeptidase, and tryptase (3). Tryptase is highly restricted to mast cells. Hence, it has been used extensively to identify mast cells, of which a subset contains MMCP-4 (3). We found ~150 tryptase$^+$ mast cells/mm^2 in the infarct/border zone of 72 h post-I/R WT hearts, of which ~50 cells/mm^2 were positive for MMCP-4 (Fig. 1*D*). By contrast, mast cells were rare (<0.01 cells/mm^2) in sham LVs or remote LVs of 72-h post-I/R mice. This difference indicates an ~15,000-fold increase in mast cell numbers in the infarct border zone by 72 h after I/R. Mast cell infiltration is regulated by stem cell factor (SCF) (13). After I/R, peak levels of SCF mRNA were found at 48 h of reperfusion (Table S1), which precedes the peak increase in MMCP-4 expression (Fig. 1*A*).

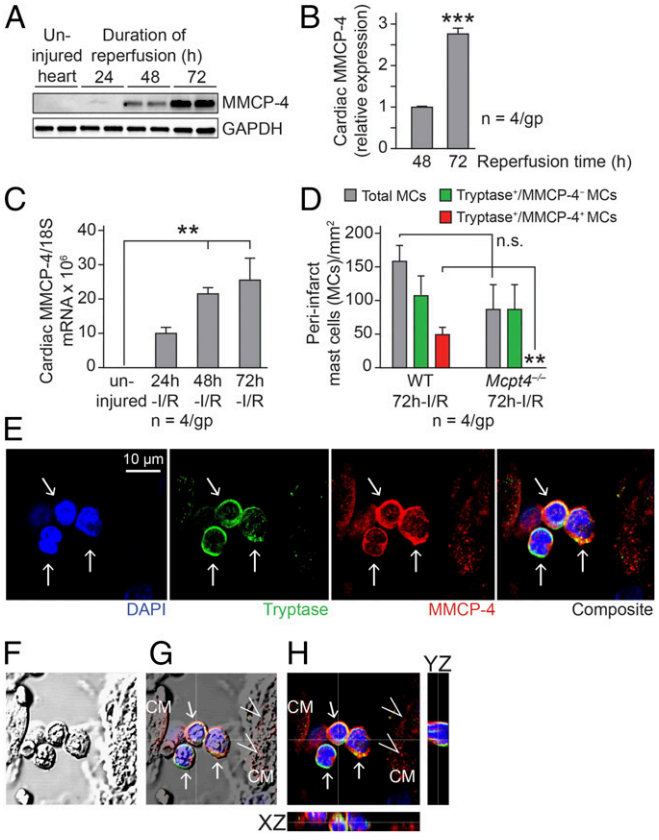

Fig. 1. MMCP-4 levels and mast cell numbers in murine hearts after I/R. (*A*) Immunoblot showing MMCP-4 in uninjured WT LVs and in 24- to 72-h post-I/R hearts. (*B*) Quantitation of MMCP-4 protein in 48- and 72-h post-I/R hearts. (*C*) MMCP-4 mRNA levels in uninjured WT and 24- to 72-h post-I/R hearts. (*D*) Tryptase$^+$/MMCP-4$^-$ and tryptase$^+$/MMCP-4$^+$ mast cells in the infarct/border zone of 72-h post/I/R WT and *Mcpt4*$^{-/-}$ hearts. *n*, number of individual animals studied; data are mean ± SEM $^{**}P < 0.01$; $^{***}P < 0.001$; n.s., not significant. (*E*) A photomicrograph showing a cluster of tryptase$^+$ (green) cells (tryptase staining identifies mast cells) in the infarct border zone of a 72-h post-I/R WT heart. Nuclei are stained with DAPI (blue) and MMCP-4 staining is in red. Arrows indicate tryptase$^+$ mast cells that also have cytoplasmic MMCP-4 staining. Images in *E* (from left to right) show DAPI, tryptase, MMCP-4 staining, and the *Right* shows a composite image. (*F*) Differential interference contrast (DIC) image of tissue section in *E*. (*G*) Overlay of composite image in *E* and DIC image in *F* showing MMCP-4$^+$ mast cells (arrows). Adjacent to these cells, diffuse MMCP-4 staining is seen on cardiomyocytes (CMs) (arrowheads). (*H*) YZ and XZ planes showing cytoplasmic MMCP-4 and tryptase staining in interstitial cells and diffuse staining over CMs in the XZ plane.

In humans, chymase is mainly found in mast cells, but endothelial cells also contain limited amounts of this protease (3). To our knowledge, however, MMCP-4 is predominantly (if not exclusively) expressed by mast cells; this contention is supported by the finding that MMCP-4 mRNA is low but detectible in heart and blood vessels of WT, but not mast cell-deficient, mice (8, 14). Moreover, in vivo, provoked release of MMCP-4 into the cardiac interstitium is lost in mast cell-deficient mice (8). Although our studies cannot rigorously exclude extramast cell production of MMCP-4, XY and XZ reconstruction planes of confocal images of 72-h post-I/R heart sections showed cytoplasmic MMCP-4 staining only in interstitial cells, identified as mast cells because of tryptase staining (Fig. 1 *E*–*H*). However, in cells adjacent to these MMCP-4$^+$ cells—such as cardiomyocytes—we often observed diffuse cell surface MMCP-4 staining (Fig. 1*G*).

Next we investigated the role of the *Mcpt4* gene in I/R-induced changes in cardiac structure and function. Comparison of 12-wk-old WT and *Mcpt4*$^{-/-}$ mice revealed no significant baseline differences in heart rate, blood pressure, LV end-systolic, and end-diastolic dimensions or ejection fraction (LVEF) (Table S2). However, 2 wk after I/R, LVEF was 26% greater in *Mcpt4*$^{-/-}$ mice compared with WT controls (Fig. 2*A*); this improvement was accompanied by reduced LV dilatation with decreases in end-systolic and -diastolic volumes (Fig. 2*B*) and attenuated infarct expansion (regional wall thinning) (Fig. 2*C*). I/R-induced cardiomyocyte hypertrophy (in the remote LV) and LV fibrosis were also reduced by *Mcpt4* deletion (Fig. 2 *D* and *E*). MMCP-4–dependent Ang II generation in blood vessels regulates blood pressure in an experimental model of renovascular hypertension (14). We investigated whether post-I/R differences in afterload could account for different outcomes between genotypes. However, this explanation was not supported by the finding of similar mean arterial blood pressures in 14-d post-I/R WT and *Mcpt4*$^{-/-}$ mice (Fig. 2*F*). Together, these studies indicate that *Mcpt4* gene expression mediates adverse functional and structural changes in the heart after I/R.

Beneficial Effects of *Mcpt4* Deletion in Postischemic Hearts Are Independent of RAS Blockade. Serine proteases of mast cells and neutrophils, particularly chymase and cathepsin G, convert Ang I to Ang II (3, 15). These proteases collectively form ACE-independent, alternative pathways for Ang II generation, and both are insensitive to ACE inhibitors (ACEi). Because both mast cells and neutrophils infiltrate the I/R damaged heart in large numbers, alternate pathways of Ang II generation must be considered in the pathogenesis of postischemic heart disease.

To this end, we compared ACEi monotherapy (captopril) with triple therapy (AAA); the latter involving a combination of an ACEi (captopril) plus a type I (AT_1) (valsartan) and a type 2 (AT_2) Ang II receptor blocker (PD122139). ACEi should prevent ACE-dependent Ang II formation, but allow MMCP-4 (or cathepsin G) dependent Ang II formation, whereas AAA therapy should inhibit actions of Ang II produced by both ACE and non-ACE pathways. WT mice were subjected to I/R, and ACEi or AAA therapy initiated 24 h after reperfusion. We found no greater improvement in LV function or dilatation after 13 d of AAA therapy than after ACEi monotherapy (Table S3), arguing against a role for non-ACE Ang II-forming pathways in post-I/R hearts.

We then addressed whether MMCP-4 has a role beyond Ang II generation in postischemic hearts. We compared LVEF after 14 d of I/R in WT and *Mcpt4*$^{-/-}$ mice, with or without AAA therapy. Whereas LVEF was 1.38-fold higher in *Mcpt4*$^{-/-}$ mice treated with AAA (49 ± 2.5%, $n = 16$) than in vehicle controls (35.6 ± 2.6%; $n = 20$; $P < 0.001$ by two-way ANOVA/Tukey multiple comparisons test), this difference did not reach significance ($P > 0.05$) compared with the increment (1.29-fold) in

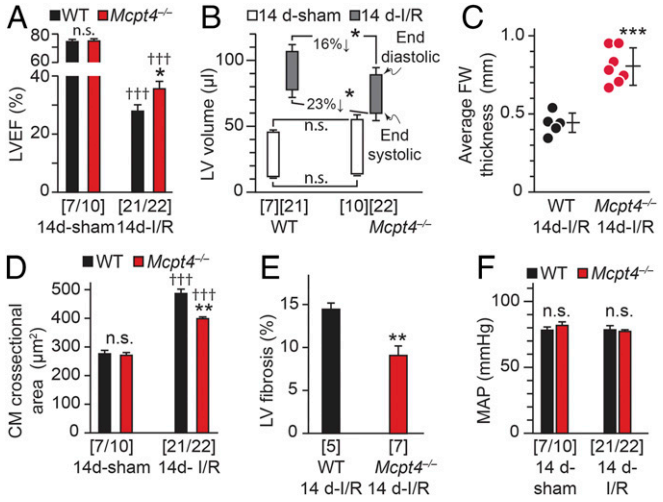

Fig. 2. Cardiac structure and function 14 d after I/R are improved by *Mcpt4* deletion. (*A* and *B*) LVEF *(A)* and end-systolic and -diastolic LV volumes (*B*) in WT and *Mcpt4*$^{-/-}$ mice. (*C*) Average free wall (FW) thickness of WT and *Mcpt4*$^{-/-}$ hearts. (*D* and *E*) Cardiomyocyte cross-sectional area (in the remote myocardium) (*D*) and LV fibrosis (*E*) in WT and *Mcpt4*$^{-/-}$ hearts. (*F*) Mean arterial blood pressures (MAP) in mice 14 d after I/R or sham surgery. Values in square brackets are the number of animals studied; data are mean ± SEM **P* < 0.05; ***P* < 0.01; ****P* < 0.001; n.s., not significant for intergenotype comparisons. †††*P* < 0.001 for intragenotype comparisons in *A* and *D*.

LVEF in WT mice treated with AAA versus vehicle controls (28.3 ± 1.8%, $n = 21$, versus 36.6 ± 2.6%, $n = 14$, in vehicle- and AAA-treated mice, respectively). In contrast, the difference in LVEF (1.34-fold) between AAA-treated *Mcpt4*$^{-/-}$ mice and AAA-treated WT mice was significant ($P < 0.01$). Thus, after I/R, functional benefits of MMCP-4 suppression are observed even in the face of RAS blockade and are, thus, mechanistically RAS-independent.

***Mcpt4* Deletion Decreases Late but Not Early Infarct Size in Post-I/R Hearts.** Postischemic cardiac dysfunction and remodeling are intimately linked to infarct size (16). In pig hearts subjected to ischemia, and then perfused for approximately 2 h, chymase inhibitor treatment reduced infarct size as assessed by serum troponin levels or infarct size relative to the area at risk (17). We investigated whether MMCP-4 deficiency influences post-I/R infarct development. In mice, unlike pigs, 24 h post-I/R infarct size, estimated by 2,3,5-triphenyltetrazolium chloride (TTC)-staining (Fig. 3*A*) or serum cardiac troponin I levels (Fig. 3B) was not significantly different between WT and *Mcpt4*$^{-/-}$ mice. Moreover, the absence of a significant difference in the area at risk between genotypes (Fig. 3*A*) at 24 h after I/R suggests that the lack of effect of *Mcpt4* deletion on early infarct size was not complicated by intergenotype differences in the baseline architecture of the LV coronary microcirculation.

MMCP-4 expression is increased 48–72 h after I/R (Fig. 1 *A* and *B*). To test whether MMCP-4 deficiency impacts late infarct size, which encompasses the period of increased MMCP-4 expression, we studied mice after 14 d of reperfusion. In contrast to the effect of MMCP-4 deletion on early infarct area, *Mcpt4*$^{-/-}$ deletion markedly reduced (by ~50%) 14 d post-I/R LV scar area (Fig. 3 *C* and *D*). This decrease was not related to differences in infarct border zone capillary density, which was similar in WT and MMCP-4–deficient mice (Fig. 3*E*).

The decreased scar area (Fig. 3 *C*–*E*) in MMCP-4–deficient hearts is consistent with improved function (Fig. 2 *A*–*C*) and could be due to late preservation of myocardium after I/R through a suppression of deleterious effects of MMCP-4 on cardiomyocyte survival. We considered this possibility because prior in vitro work has shown that mast cell serine proteinases cause cultured rat neonatal cardiomyocyte to undergo apoptosis (18); albeit that the apoptosis mechanism was not explored.

We explored the previously unidentified hypothesis that MMCP-4 mediates late myocardial cell death in post-I/R hearts by degrading IGF-1. Three lines of evidence led us to formulate this hypothesis: (*i*) cardiac IGF-1 mRNA expression is markedly, but transiently, increased 24–72 h after a MI (19); (*ii*) IGF-1 has a key role in the regulation of cell survival in general, and in the setting of MI, exogenous administration of IGF-1 attenuates cardiac dysfunction and reduces infarct size (10), and (*iii*) there are several predicted MMCP-4 sensitive cleavage sites in mouse IGF-1—based on the extended substrate binding specificity of MMCP-4 (20)—suggesting that MMCP-4 could be an IGF-1–degrading enzyme.

MMCP-4 Is the Major IGF-1–Degrading Enzyme in 72-h Post-I/R Hearts. We found that IGF-1–degrading activity in 72-h post-I/R heart homogenates is associated with a charged soluble chymotrypsin-like serine protease, based on its extraction from crude membrane/extracellular matrix pellet fractions by high KCl concentrations, and its inhibition by phenylmethylsulfonyl fluoride and chymostatin (Fig. 4 *A* and *B*)—biochemical properties common to most chymases (4). Moreover, IGF-1–degrading activity in the high salt extract of 72-h post-I/R LVs was inhibited by an affinity-purified polyclonal antibody raised against a unique MMCP-4 epitope (Fig. 4*B*) (8).

Further support for MMCP-4 being an IGF-1–degrading enzyme is the finding that in vitro purified MMCP-4 degrades mouse IGF-1 (Fig. 4*C*), and human chymase degrades human-IGF-1 (Fig. 4*D*). Notably, IGF-1–degrading activity was prominently observed in 72 h post-I/R WT, but not in *Mcpt4*$^{-/-}$ heart homogenates (devoid of protease inhibitors). Moreover, immunoblots revealed a band at 30 kDa (which is the molecular mass of native MMCP-4) and a 19-kDa degradation product in WT but not MMCP-4–deficient heart homogenates (Fig. 4*E*). The 19-kDa MMCP-4 fragment is likely to occur by autocatalysis as we have

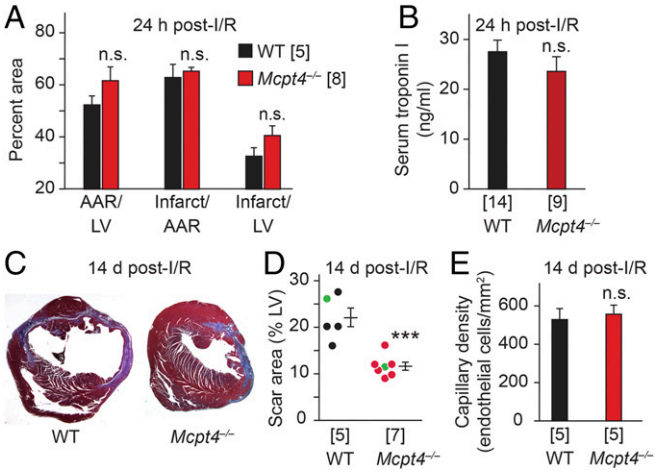

Fig. 3. Late, but not early, infarct size after I/R is reduced by *Mcpt4* deletion. (*A*) Area at risk (AAR) and infarct size expressed as a percentage of LV volume. Data are from 24-h post-I/R WT and *Mcpt4*$^{-/-}$ hearts. (*B*) Serum troponin I levels in 24-h post-I/R WT and *Mcpt4*$^{-/-}$ mice. *n* is the number of biological replicates (in square brackets); data are and mean ± SEM; n.s., not significant. (*C*) Heart sections at comparable levels of 14-d post-IR WT or *Mcpt4*$^{-/-}$ mice. Collagen in scar is blue and myocytes are red. (*D*) Scar area in WT and *Mcpt4*$^{-/-}$ post-I/R hearts was calculated in each of five sequential 500-μm LV sections. The average value is shown. The green data points are from the representative hearts shown in *C*. (*E*) Peri-infarct capillary density in 14-d post-I/R WT and *Mcpt4*$^{-/-}$ hearts. Values in square brackets are the number of animals studied; data are mean ± SEM, **P* < 0.05; ****P* < 0.001; n.s., not significant.

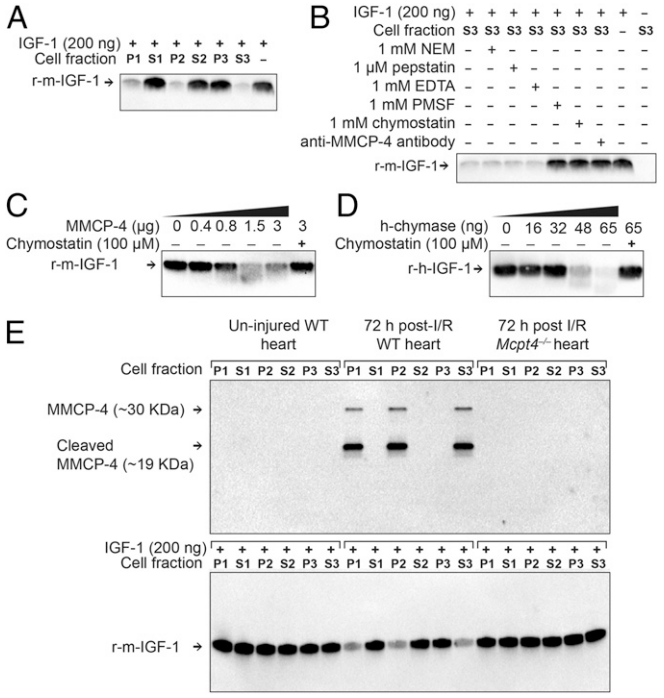

Fig. 4. Identification of MMCP-4 as the major IGF-1–degrading protease in post-I/R hearts. (*A*) Fractionated 72-h post-IR WT heart was incubated with recombinant mouse IGF-1 (r-m-IGF-1) and then subjected to SDS/PAGE and immunoblotting. S1 and P1 are high-speed supernatant fraction and membrane pellet, respectively. S2 and P2 are 1% Triton X-100 supernatant fraction and pellet, respectively, derived from P1. S3 and P3 are 1 M KCl supernatant fraction and pellet, respectively, derived from P2. Soluble r-m-IGF-1–degrading activity is evident in the high KCl extract, S3. (*B*) Immunoblot showing that IGF-1–degrading activity in S3 is resistant to cysteine-(*N*-ethylmaleimide, NEM), aspartyl- (pepstatin), or metalloproteinase (EDTA) inhibition, but is inhibited by the pan-serine protease inhibitor, phenylmethylsulfonyl fluoride (PMSF), the chymotrypsin-like protease inhibitor, chymostatin, or an affinity-purified antibody raised against a unique MMCP-4 peptide fragment (9). Blot shown is representative of three independent studies. (*C*) Concentration-dependent cleavage of r-m-IGF-1 by purified MMCP-4. (*D*) Concentration-dependent cleavage of recombinant human IGF-1 (r-h-IGF-1) by recombinant human chymase. IGF-1 degradation in *C* and *D* was inhibited by chymostatin, indicating that cleavage is by a chymotrypsin-like protease. Immunoblots in *C* and *D* are representative of four independent studies for each enzyme–substrate pair. (*E*) Hearts from uninjured WT, 72-h post-I/R WT, and 72-h post-I/R *Mcpt4*$^{-/-}$ mice were subjected to tissue fractionation as in *A*. Aliquots of the P1, S1, P2, S2, P3, and S3 fractions were used to determine MMCP-4 level by immunoblotting (*Upper*) and assayed for IGF-1–degrading activity (*Lower*).

demonstrated with human chymase (4). Together, these findings suggest that the major IGF-1–degrading activity in 72 h post-I/R hearts is due to MMCP-4.

I/R Increases IGF-1 Expression in Hearts. IGF-1 mRNA levels were unchanged initially, but increased markedly between 48 and 72 h after I/R in WT hearts (Table S4). In 72-h post-I/R hearts, IGF-1 mRNA was enriched in cardiomyocytes (relative expression: 1 ± 0.22 versus 0.27 ± 0.027 ^{18}S-normalized IGF-1 mRNA transcripts in cardiomyocytes and noncardiomyocytes, respectively, $n = 3$, $P < 0.05$), suggesting that these cells are the main source of IGF-1 production. In contrast to IGF-1 mRNA levels, cardiac IGF-1 protein levels fell by 35% between 48 and 72 h after I/R ($P < 0.001$) (Fig. 5*A*). Fig. 5*B* presents examples of the immunohistochemical localization of IGF-1 in uninjured and post-I/R hearts. The findings of reciprocal changes in IGF-1 protein and its mRNA, marked increases in MMCP-4 levels in 72-h post-I/R hearts (Fig. 1 *A* and *B*), and the discovery of MMCP-4's potent IGF-1 degrading activity (Fig. 4*C*) indicate posttranslational regulation of cardiac IGF-1 by MMCP-4.

MMCP-4 Regulates Cardiac IGF-1 and IGF-1/IGF-1R Signaling Post-I/R. Consistent with MMCP-4 regulating cardiac IGF-1 levels and prosurvival IGF-1 signaling in vivo, cardiac IGF-1 levels were 1.7-fold higher in 72-h post-I/R *Mcpt4*$^{-/-}$ mice than in WT controls (Fig. 6*A*). We ruled out increased IGF-1 mRNA expression or increased endocrine input of IGF-1 to *Mcpt4*$^{-/-}$ hearts, as explanations, because, at 72 h after I/R, neither cardiac IGF-1 mRNA nor serum IGF-1 levels were increased by *Mcpt4* deletion (Table S5).

IGF-1 controls cell survival by activating the insulin receptor substrate (IRS)-1/phosphoinositide 3 kinase/Akt and IRS-2/MEK/ERK effector pathways (21). Despite a lack of change in IGF-1R mRNA expression (relative expression: 1 ± 0.19 versus 1.19 ± 0.14 in 72-h post-I/R WT and *Mcpt4*$^{-/-}$ hearts, respectively; $n = 4$ per group; $P = 0.39$), *Mcpt4* deletion increased the abundance of phosphorylated Akt-S473 and phosphorylated ERK-1/2 in 72-h post-I/R hearts (Fig. 6*A*). Phosphorylation of BAD at S136 by Akt, and at S112 by ERK, inhibits BAD's proapoptotic effects (22). *Mcpt4* deletion increased phosphorylation of BAD at both S112 and S136 (Fig. 6*A*). It also increased CREB phosphorylation and Bcl-2 levels (Fig. 6*A*), and reduced caspase-3 activation and decreased cleavage of the DNA repair enzyme poly ADP ribose polymerase (PARP) (Fig. 6*A*)—a target of caspase-3.

To determine whether the inverse changes in IGF-1 and activated caspase-3 caused by *Mcpt4* deletion are causally related, we pretreated (for 8 h from 64 to 72 h after I/R) *Mcpt4*$^{-/-}$ mice with the specific IGF-1R inhibitor, picropodophyllin (PPP) (23). Hearts were then harvested at 72 h after I/R. This acute IGF-1R inhibition caused an ~2.5-fold activation of cardiac caspase-3 ($P < 0.001$) (Fig. 6*B*), consistent with IGF-1/IGF-1R signaling in post-I/R *Mcpt4*$^{-/-}$ hearts being prosurvival. Consistent with reduced

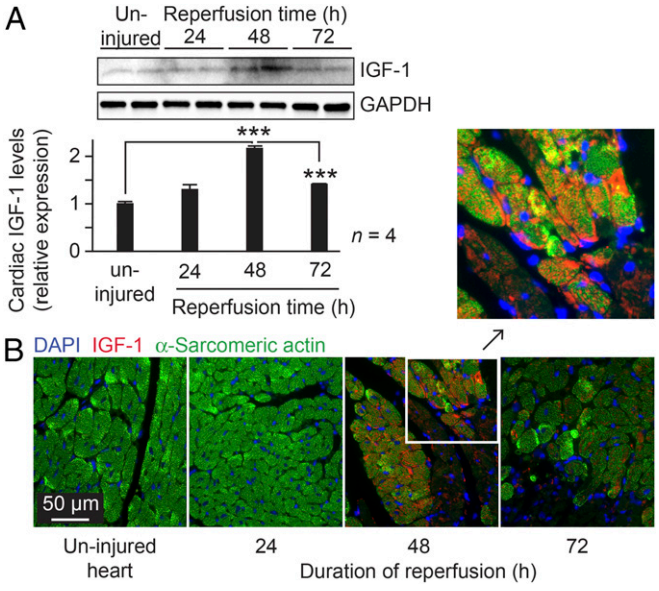

Fig. 5. Increased IGF-1 expression in post-I/R hearts. (*A*) Representative immunoblots and quantitative assessment of IGF-1 expression in uninjured WT hearts and in 24- to 72-h post-I/R hearts. Data are mean ± SEM; the data were normalized by using GAPDH as loading controls and values are relative to IGF-1 levels in uninjured hearts. ***$P < 0.001$. (*B*) Immunofluorescent images depict cardiomyocytes expressing α-sarcomeric actin (green), IGF-1 (red), and nuclei (blue) in sections from uninjured WT or 24- to 72-h post-I/R hearts. *Inset* shows a magnified view of the white box. The scale bar is the same for all images. Images are representative of four hearts at each time point.

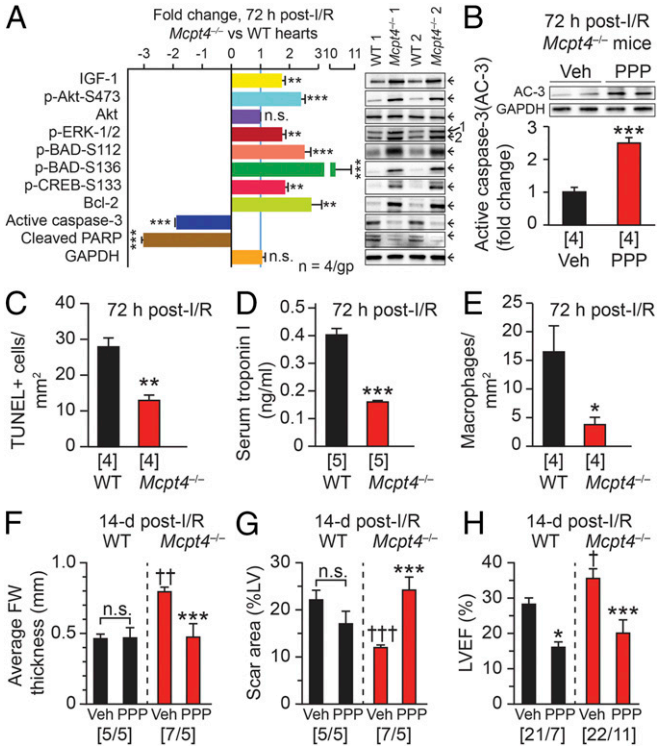

Fig. 6. *Mcpt4* deletion increases IGF-1–dependent prosurvival signaling after I/R and improves cardiac structure and function. (*A*) IGF-1 and prosurvival IGF-1 signaling protein levels in *Mcpt4*$^{-/-}$ and WT hearts 72 h after I/R. Representative immunoblots are on the right. Data are from four independent biological replicates. (*B*) Acute inhibition of IGF-1R by PPP (for 8 h) increases caspase-3 activation in 72 h post-I/R *Mcpt4*$^{-/-}$ hearts. (*C–E*) Apoptotic (TUNEL^{+}) cells (*C*), serum troponin I levels (*D*), and macrophages (*E*) in the infarct border zone of WT or *Mcpt4*$^{-/-}$ mice 72 h after I/R. Data are mean ± SEM, $*P < 0.05$; $**P < 0.01$; $***P < 0.001$. (*F–H*) Effect of IGF-1/IGF-1R inhibition by PPP (starting at 24 h after reperfusion and continuing until 14 d after I/R) on LV free wall (FW) width (*F*), scar area (*G*), and LVEF (*H*) in WT and *Mcpt4*$^{-/-}$ mice. In these graphs, the vehicle data are from Figs. 2 and 3. Values in square brackets are the number of independent biological replicates. $*P < 0.05$; $***P < 0.001$; n.s., not significant for differences between treatment groups and $\dagger P < 0.05$; $\dagger\dagger P < 0.05$; $\dagger\dagger\dagger P < 0.001$ for intergenotype differences.

cardiomyocyte death and tissue injury, compared with WT controls, there were twofold fewer apoptotic cells (TUNEL staining) in the infarct border zone of 72-h post-I/R *Mcpt4*$^{-/-}$ hearts (Fig. 6*C*), serum cardiac troponin I levels were reduced by 60% in 72-h post-I/R *Mcpt4*$^{-/-}$ mice (Fig. 6*D*), and macrophage infiltration in the infarct border zone was reduced by 77% (Fig. 6*E*).

Mcpt4 deletion reduces kidney TNFα and MCP1, but not IL1β or TGFβ, mRNA in experimental chronic kidney disease, suggesting that MMCP-4 is proinflammatory (24). We found no significant differences in serum TNFα, MCP1, IL1β, and TGFβ between 72-h post-I/R WT and *Mcpt4*$^{-/-}$ mice (Table S6). Seventy-two-hour post-I/R cardiac TNFα, MCP1, and IL1β mRNA levels were also not significantly affected by *Mcpt4* deletion, but TGFβ mRNA levels decreased by ∼50% ($P < 0.01$) (Table S6). This decrease was not reversed by acute 8-h IGF-1R inhibition (using PPP) (Table S7), suggesting that IGF-1R signaling does not regulate TGFβ mRNA levels in post-I/R *Mcpt4*$^{-/-}$ hearts. TGFβ is profibrotic. Hence, fibrosis reduction in *Mcpt4*$^{-/-}$ hearts might, in part, be due to reduced TGFβ mRNA levels.

Collectively, our findings indicate that the deleterious effects of MMCP-4 after I/R are independent of its Ang II-forming activity, but rather are mediated by its IGF-1–degrading activity, which abolishes the late beneficial effects provided by enhanced IGF-1R prosurvival signaling. To further confirm this notion, we studied whether chronic IGF-1/IGF-1R inhibition abolishes all, or some, of the post-I/R protection afforded by *Mcpt4* deletion. We found that although *Mcpt4* deletion attenuated infarct expansion (wall thinning) at 14 d after I/R, this salutary effect was prevented by chronic IGF-1/IGF-1R inhibition (from 24 h to 14 d after I/R) (Fig. 6*F*). By contrast, chronic IGF-1/IGF-1R inhibition with PPP had no significant effect on infarct expansion in WT hearts (Fig. 6*F*). Similarly, after chronic IGF-1/IGF-1R inhibition, 14-d post-I/R scar areas in both WT and *Mcpt4*$^{-/-}$ mice were not significantly different from those in untreated WT controls (Fig. 6*G*) but, in the absence of IGF-1R inhibition, were smaller in *Mcpt4*$^{-/-}$ mice (Fig. 3*D*). Thus, endogenous IGF-1 activation does not protect ischemia-injured WT hearts from late infarct progression, but when MMCP-4 (and its IGF-1–degrading activity) is deleted, IGF-1 increases to a level that suppresses late infarct progression.

We also studied LV systolic function in these mice (Fig. 6*H*) and found that chronic IGF-1/IGF-1R inhibition markedly decreased LVEF in both WT and *Mcpt4*$^{-/-}$ mice to about the same level. Because LVEF was greater in post-I/R *Mcpt4*$^{-/-}$ mice than in WT controls, IGF-1R inhibition produced a greater decrease in LV systolic function in *Mcpt4*$^{-/-}$ mice. Together, these data suggest that, in WT animals, late post-I/R induction of endogenous IGF-1 is sufficient to impact cardiac function (Fig. 6*H*), but not infarct progression (Fig. 6 *F* and *G*). By decreasing IGF-1 cleavage, *Mcpt4* deletion increases endogenous IGF-1 levels and prosurvival signaling to a level that allows late cardioprotection, which inhibits infarct progression.

Discussion

Exogenous IGF-1 inhibits apoptosis in reperfused hearts after an ischemic injury, as well as improving LV function and reducing adverse cardiac remodeling (9–11). IGF-1 plays critical roles in fetal and early postnatal heart growth (25, 26), but its expression is repressed soon after birth. The evidence presented here indicates that a few days after the start of reperfusion, myocardial IGF-1 levels increase, which could potentially limit further cardiomyocyte loss by inhibiting caspase-3 activation (21). However, our data suggest, rather, that post-I/R increases in cardiac MMCP-4 (most likely due to infiltration of MMCP-4 containing mast cell into the infarct zone) degrades IGF-1 and, thus, antagonizes its prosurvival effects, resulting in enhanced apoptosis and late infarct progression. Although cardiac dysfunction is related to infarct size in postischemic hearts (16), our results suggest that some of the functional effects of endogenous IGF-1 may be independent of its cardioprotective effects. This explanation is based on the finding that IGF-1/IGF-1R inhibition in post-I/R WT mice exacerbated LV systolic dysfunction without impacting late infarct progression. Whether this increased dysfunction is caused by blockade of a direct effect of IGF-1 on cardiomyocyte contractility, or involves other known effects of IGF-1—e.g., on cardiomyocyte metabolism, hypertrophy, autophagy, and replication (21)—remains to be established.

Mcpt4 deletion produced a relatively small (∼25%) improvement in post-I/R LV systolic function (Fig. 2*A*). Although even modest improvements can be important in human MI, the increase in systolic function in *Mcpt4*$^{-/-}$ mice is achieved at lower LV end-diastolic and -systolic volumes and at higher LV wall thicknesses, which are likely attributable to amelioration of pathological remodeling. Wall stress is proportional to LV chamber diameter and inversely proportional to wall thickness (27). Thus, *Mcpt4* deletion likely lowers wall stress in post-I/R hearts at a time when systolic function is modestly improved; a reduction in wall stress is expected to increase mechanical efficiency of ischemia-injured hearts. Future studies are needed to understand whether chymase inhibitors improve post-MI survival by this mechanism (7, 8).

Clinical studies have established an important deleterious effect of Ang II in postischemic heart disease (2). Studies with

chymase inhibitors have often alluded to the Ang II-forming activity of chymase as being critical to its detrimental effect in postischemic hearts—based entirely on associative findings (e.g., ref. 28). We show that whereas *Mcpt4* deletion improves cardiac structure and function post-I/R, this effect is unrelated to blockade of a non-ACE Ang II-forming pathway. Chymases activate promatrix metalloproteinase 2 and 9 (pro-MMP2/9) (29), which could promote wall thinning and cardiac dilatation by degrading the cardiac interstitial matrix. Regional wall thinning is a consequence of myofiber slippage (30), and MMP-dependent extracellular remodeling is required for continued expansion of the healing infarct (31) and chamber dilatation (32). We show that *Mcpt4* deletion attenuates infarct expansion; because this effect is negated by inhibition of IGF-1/IGF-1R signaling, it suggests that if MMCP-4–mediated pro-MMP2/9 activation is also important in post-I/R infarct progression, it is indirect and involves IGF-1.

MMCP-4 is the functional homolog of human chymase (e.g., ref. 8). We show here that, like MMCP-4, human chymase also degrades IGF-1. The rationale for developing human chymase inhibitors was to prevent chymase-mediated Ang II formation, which is resistant to ACE inhibition. However, a double-blind trial showed little improvement when AT_1 receptor blockade was combined with ACEi treatment versus ACEi monotherapy (2). This lack of difference provided an argument against the use of chymase inhibitor therapy in patients with MI. We believe that this trial actually left unresolved the question of whether direct chymase inhibition, independent of its effects on Ang II generation, might be effective in these patients. Given the findings here, it is likely that chymase inhibitors may prove to be useful for protecting patients from delayed post-I/R cardiac injury and therefore warrant clinical investigation.

Materials and Methods

Animals were handled according to Emory University's Institutional Animal Care and Use Committee (IACUC) Guidelines. To minimize inbred strain background effects, $Mcpt4^{-/-}$ mice (33) were first backcrossed for >12 generations to the C57BL/6J genetic background. Then, fewer than five homozygote × homozygote $Mcpt4^{-/-}$ crosses or WT × WT C57BL/6J mice crosses were used to accumulate $Mcpt4^{-/-}$ or WT homozygous progeny, respectively, which were studied at 11–13 wk of age. This breeding strategy allowed a large number of mice to be rapidly generated so that I/R surgeries could be performed by one surgeon (T.T.) over a short period. I/R surgeries were performed, as described (34), in cohorts of ∼8 mice per day. Infarct size and echocardiographic analyses were performed as described (34). Protein and gene expression levels were estimated by immunoblotting and quantitative RT-PCR, respectively, and IGF-1 was visualized by immunohistochemistry using described protocols (26). Detailed material and methods are provided in *SI Materials and Methods*.

ACKNOWLEDGMENTS. This work was funded by a Department of Medicine, Emory University grant; a Carlyle Fraser Heart Center, Emory University Hospital Midtown grant; NIH Grants HL079040, HL127726, HL098481, T32HL007745, HL092141, HL093579, HL094373, and HL113452; American Heart Association Grant 13SDG16460006; a Swedish Research Council grant; the Foundation Leducq; and National Health and Medical Research Council of Australia Grant 573732.

1. Pfeffer MA, et al.; The SAVE Investigators (1992) Effect of captopril on mortality and morbidity in patients with left ventricular dysfunction after myocardial infarction. Results of the survival and ventricular enlargement trial. *N Engl J Med* 327(10):669–677.
2. Pfeffer MA, et al.; Valsartan in Acute Myocardial Infarction Trial Investigators (2003) Valsartan, captopril, or both in myocardial infarction complicated by heart failure, left ventricular dysfunction, or both. *N Engl J Med* 349(20):1893–1906.
3. Wernersson S, Pejler G (2014) Mast cell secretory granules: Armed for battle. *Nat Rev Immunol* 14(7):478–494.
4. Urata H, Kinoshita A, Misono KS, Bumpus FM, Husain A (1990) Identification of a highly specific chymase as the major angiotensin II-forming enzyme in the human heart. *J Biol Chem* 265(36):22348–22357.
5. Jin D, et al. (2003) Impact of chymase inhibitor on cardiac function and survival after myocardial infarction. *Cardiovasc Res* 60(2):413–420.
6. Kanemitsu H, et al. (2006) Chymase inhibition prevents cardiac fibrosis and dysfunction after myocardial infarction in rats. *Hypertens Res* 29(1):57–64.
7. Hoshino F, et al. (2003) Chymase inhibitor improves survival in hamsters with myocardial infarction. *J Cardiovasc Pharmacol* 41(Suppl 1):S11–S18.
8. Wei CC, et al. (2010) Mast cell chymase limits the cardiac efficacy of Ang I-converting enzyme inhibitor therapy in rodents. *J Clin Invest* 120(4):1229–1239.
9. Dai W, Kloner RA (2011) Cardioprotection of insulin-like growth factor-1 during reperfusion therapy: What is the underlying mechanism or mechanisms? *Circ Cardiovasc Interv* 4(4):311–313.
10. O'Sullivan JF, et al. (2011) Potent long-term cardioprotective effects of single low-dose insulin-like growth factor-1 treatment postmyocardial infarction. *Circ Cardiovasc Interv* 4(4):327–335.
11. Davis ME, et al. (2006) Local myocardial insulin-like growth factor 1 (IGF-1) delivery with biotinylated peptide nanofibers improves cell therapy for myocardial infarction. *Proc Natl Acad Sci USA* 103(21):8155–8160.
12. Osterziel KJ, et al. (1998) Randomised, double-blind, placebo-controlled trial of human recombinant growth hormone in patients with chronic heart failure due to dilated cardiomyopathy. *Lancet* 351(9111):1233–1237.
13. Nilsson G, Butterfield JH, Nilsson K, Siegbahn A (1994) Stem cell factor is a chemotactic factor for human mast cells. *J Immunol* 153(8):3717–3723.
14. Li M, et al. (2004) Involvement of chymase-mediated angiotensin II generation in blood pressure regulation. *J Clin Invest* 114(1):112–120.
15. Reilly CF, Tewksbury DA, Schechter NM, Travis J (1982) Rapid conversion of angiotensin I to angiotensin II by neutrophil and mast cell proteinases. *J Biol Chem* 257(15):8619–8622.
16. Kwon DH, et al. (2009) Extent of left ventricular scar predicts outcomes in ischemic cardiomyopathy patients with significantly reduced systolic function: A delayed hyperenhancement cardiac magnetic resonance study. *JACC Cardiovasc Imaging* 2(1):34–44.
17. Oyamada S, Bianchi C, Takai S, Chu LM, Sellke FW (2011) Chymase inhibition reduces infarction and matrix metalloproteinase-9 activation and attenuates inflammation and fibrosis after acute myocardial ischemia/reperfusion. *J Pharmacol Exp Ther* 339(1):143–151.
18. Hara M, et al. (1999) Mast cells cause apoptosis of cardiomyocytes and proliferation of other intramyocardial cells in vitro. *Circulation* 100(13):1443–1449.
19. Reiss K, et al. (1994) Acute myocardial infarction leads to upregulation of the IGF-1 autocrine system, DNA replication, and nuclear mitotic division in the remaining viable cardiac myocytes. *Exp Cell Res* 213(2):463–472.
20. Andersson MK, Karlson U, Hellman L (2008) The extended cleavage specificity of the rodent beta-chymases rMCP-1 and mMCP-4 reveal major functional similarities to the human mast cell chymase. *Mol Immunol* 45(3):766–775.
21. Troncoso R, Ibarra C, Vicencio JM, Jaimovich E, Lavandero S (2014) New insights into IGF-1 signaling in the heart. *Trends Endocrinol Metab* 25(3):128–137.
22. Fang X, et al. (1999) Regulation of BAD phosphorylation at serine 112 by the Ras-mitogen-activated protein kinase pathway. *Oncogene* 18(48):6635–6640.
23. Strömberg T, et al. (2006) IGF-1 receptor tyrosine kinase inhibition by the cyclolignan PPP induces G2/M-phase accumulation and apoptosis in multiple myeloma cells. *Blood* 107(2):669–678.
24. Scandiuzzi L, et al. (2010) Mouse mast cell protease-4 deteriorates renal function by contributing to inflammation and fibrosis in immune complex-mediated glomerulonephritis. *J Immunol* 185(1):624–633.
25. Xin M, et al. (2011) Regulation of insulin-like growth factor signaling by Yap governs cardiomyocyte proliferation and embryonic heart size. *Sci Signal* 4(196):ra70.
26. Naqvi N, et al. (2014) A proliferative burst during preadolescence establishes the final cardiomyocyte number. *Cell* 157(4):795–807.
27. Grossman W, Jones D, McLaurin LP (1975) Wall stress and patterns of hypertrophy in the human left ventricle. *J Clin Invest* 56(1):56–64.
28. Jin D, Takai S, Yamada M, Sakaguchi M, Miyazaki M (2002) Beneficial effects of cardiac chymase inhibition during the acute phase of myocardial infarction. *Life Sci* 71(4):437–446.
29. Tchougounova E, et al. (2005) A key role for mast cell chymase in the activation of pro-matrix metalloprotease-9 and pro-matrix metalloprotease-2. *J Biol Chem* 280(10):9291–9296.
30. Weisman HF, Healy B (1987) Myocardial infarct expansion, infarct extension, and reinfarction: Pathophysiologic concepts. *Prog Cardiovasc Dis* 30(2):73–110.
31. Mukherjee R, et al. (2003) Myocardial infarct expansion and matrix metalloproteinase inhibition. *Circulation* 107(4):618–625.
32. Ducharme A, et al. (2000) Targeted deletion of matrix metalloproteinase-9 attenuates left ventricular enlargement and collagen accumulation after experimental myocardial infarction. *J Clin Invest* 106(1):55–62.
33. Tchougounova E, Pejler G, Abrink M (2003) The chymase, mouse mast cell protease 4, constitutes the major chymotrypsin-like activity in peritoneum and ear tissue. A role for mouse mast cell protease 4 in thrombin regulation and fibronectin turnover. *J Exp Med* 198(3):423–431.
34. Bryan NS, et al. (2007) Dietary nitrite supplementation protects against myocardial ischemia-reperfusion injury. *Proc Natl Acad Sci USA* 104(48):19144–19149.